

D-Lite: Navigation-Oriented Compression of 3D Scene Graphs under Communication Constraints

Yun Chang^{1,*}, Luca Ballotta^{2,*}, Luca Carlone¹

Abstract—For a multi-robot team that collaboratively explores an unknown environment, it is of vital importance that collected information is efficiently shared among robots in order to support exploration and navigation tasks. Practical constraints of wireless channels, such as limited bandwidth and bit-rate, urge robots to carefully select information to be transmitted. In this paper, we consider the case where environmental information is modeled using a *3D Scene Graph*, a hierarchical map representation that describes geometric and semantic aspects of the environment. Then, we leverage graph-theoretic tools, namely *graph spanners*, to design heuristic strategies that efficiently compress 3D Scene Graphs to enable communication under bandwidth constraints. Our compression strategies are *navigation-oriented* in that they are designed to approximately preserve shortest paths between locations of interest, while meeting a user-specified communication budget constraint. The effectiveness of the proposed algorithms is demonstrated in synthetic robot navigation experiments in a realistic simulator. A video abstract is available at <https://youtu.be/nKYXU5VC6A8>.

Index Terms—Communication constraints, 3D Scene Graphs, graph spanners, multi-robot navigation, resource allocation.

I. INTRODUCTION

In the near future, robot teams will perform coordinated and cooperative tasks in various application scenarios, ranging from exploration of subterranean environments, to search-and-rescue missions in hazardous settings, to human assistance in houses, airports, factory floors, and malls, to mention a few.

A key requirement for coordinated exploration and navigation in an initially unknown environment is to build a map model of the environment as the robots explore it. Recent work has proposed *3D Scene Graphs* as an expressive hierarchical model of complex environments [1–6]: a 3D Scene Graph organizes spatial and semantic information, including objects, structures (e.g., walls), places (i.e., free-space locations the robot can reach), rooms, and buildings into a graph with multiple layers corresponding to different levels of abstraction. 3D Scene Graphs provide a user-friendly model of the scene that can support the execution of high-level instructions by a human; moreover they capture traversability between places, room, and buildings that can be readily used for path planning.

Scaling up from single-robot to multi-robot systems, a key challenge is to share the map information among the robots in

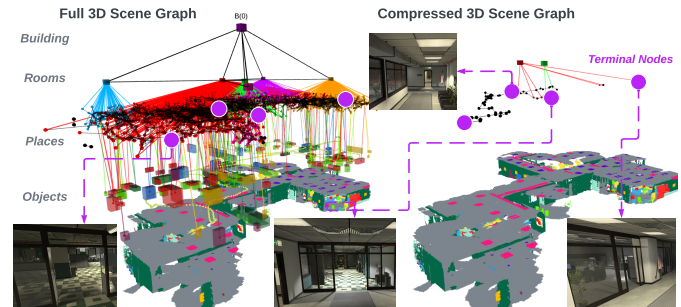


Figure 1: 3D Scene Graph of an environment (left) and compressed version produced by D-Lite (right). The purple circles mark the *terminal nodes*: D-Lite approximately preserves shortest path lengths between those locations of interest.

the team to support coordination. For instance, the robots may exchange partial maps such that a robot can more efficiently navigate within a portion of the environment mapped by another robot. However, the potentially high volume of data to be transferred over a shared wireless channel can easily saturate the available bandwidth, degrading team performance. This is particularly relevant when the map is modeled as a 3D Scene Graph, since these are rich and potentially large models if all the nodes and edges are retained. On the other hand, 3D Scene Graphs also provide opportunities to compress information: for instance, the robots may exchange information about rooms in the environment rather than sharing fine-grained traversability information encoded by the places layer; similarly, for a large-scale scene, the robot may just specify a sequence of buildings to be traversed, abstracting away low-level geometric information. This is not dissimilar from what humans do: when providing instructions to another person about how to navigate to a location in a building, we would specify a sequence of rooms and landmarks (e.g., objects or structures) rather than communicating a detailed metric map or a precise path.

Therefore, the question we address in this paper is: *how can we compress a 3D Scene Graph to retain relevant information the robots can use for navigation, while meeting a communication budget constraint, expressed as the maximum size of the map the robots can transmit?* Besides multi-robot communication, task-driven map compression may play a role in long-term autonomy of resource-constrained robots, where the robots might be unable to store a very large-scale map due to memory constraints and can only retain key aspects of it.

Related work. Graph compression is active area of research in discrete mathematics, computer science, and telecommunications, where it finds applications to, e.g., vehicle routing [7, 8], packet routing in wireless networks [9], and compression of

This work was partially funded by ARL DCIST CRA W911NF-17-2-0181, ONR RAIDER N00014-18-1-2828, Lincoln Laboratory’s Resilient Perception in Degraded Environments program, the CARIPARO Foundation Visiting Programme “HiPeR”, and the Italian Ministry of Education under the initiative “Departments of Excellence” (Law 232/2016).

¹Laboratory for Information & Decision Systems (LIDS), Massachusetts Institute of Technology, Cambridge, MA, USA, {yunchang, lcarlone}@mit.edu.

²Department of Information Engineering, University of Padova, Padova, Italy, ballotta@dei.unipd.it. *Equal contribution.

unstructured data such as 3D point clouds [10–12].

A prominent body of works aims to simplify an input graph by carefully pruning it based on structural properties of the graph. These methods typically entail some information loss, and aim to only retain relevant information when storing, processing, parsing, or transmitting the full graph is infeasible. For example, references [9, 13] find efficient representations of huge web and communication networks by heuristically selecting a few key elements, while the work [14] prunes graphs while preserving connectivity among nodes. Within the discrete mathematics literature, graph compression has been studied with attention to ensuring low distortion (or *stretch*) of inter-node distances. For example, *spanning trees* and *Steiner trees* are the smallest subgraphs ensuring connectivity in undirected graphs [15, 16]. Conversely, *graph spanners* aim to remove edges while allowing for a user-defined maximum distortion of shortest paths [17–19]. A special case of the latter are *distance preservers* [20], that prune graphs but keep shortest paths for specified node pairs. Conversely, *emulators* replace a large number of edges with a few strategic ones to ensure small stretch of distances among nodes [21].

On the other hand, lossless compression strategies aim to find compact representations of graphs to be efficiently stored or processed. A subset of related work directly deals with communication-efficient re-labeling of nodes that enhance graph encoding. For example, some classical methods exploit algebraic tools such as spectral decomposition of the incidence or adjacency matrix that allow encoding the latter with a limited number of codewords, while paper [22] proposes an algorithm that exploits graph structures such as hubs and spokes. A recent survey of lossless compression techniques is given in [23]. A different paradigm for lossless compression is based on hypergraphs, which generalize standard graphs by allowing hyperedges that connect more than two nodes. Among others, paper [24] tailors semantic data compression, [25] proposes a procedure to construct hypergraphs from network data, [26, 27] tackle hypergraph partitioning, and [28] presents a signal processing framework based on hypergraphs.

Related work in robotics has put more emphasis on graph compression to speed up path planning and decision-making algorithms. For instance, Silver *et al.* [29] exploit Graph Neural Networks to detect key nodes by learning heuristic importance scores. Agia *et al.* [30] propose an algorithm that exploits the 3D Scene Graph hierarchy to prune nodes and edges not relevant to the robotic task. Targeting a related application domain, Tian *et al.* [31] study computation and communication efficiency of multi-robot loop closure, providing a strategy to share a limited number of visual features in multi-robot SLAM and Denniston *et al.* [32] introduced a graph based method to prune the multi-robot loop closures in order to save on processing time. Finally, the line of work [33–36] proposes algorithms to derive hierarchical abstractions of tree-structured representations, for instance enabling fast planning on occupancy grid maps at progressively increasing resolution.

Novel contribution. In this paper, we tackle the challenging problem of efficiently sharing 3D Scene Graphs for navigation

under hard communication constraints. In particular, we propose two greedy algorithms, BUD-Lite and TOD-Lite (collectively referred to as *D-Lite*), that leverage graph spanners to prune nodes and edges from a given 3D Scene Graph while minimizing the distortion of the shortest paths between locations of interest (the *terminal nodes*, see Fig. 1). Differently from the literature, our algorithms (i) are designed to retain navigation-relevant information, (ii) leverage the hierarchical structure of the 3D Scene Graph for compression, and (iii) enforce a user-specified size of the compressed 3D Scene Graph. Our algorithms are computationally efficient and apply to general graphs. Furthermore, we allow for loose specifications of navigation tasks, to make our approach flexible to inexact or uncertain queries: for instance, a querying robot requesting a map from another robot may specify a number of potential location it has to navigate between, and this information is used by the queried robot for more effective 3D Scene Graph compression. To meet a sharp budget on transmitted information, we design suitable heuristics that exploit a graph spanner of the 3D Scene Graph to be sent: graph spanners allow to trade-off the size of a sub-graph of the 3D Scene Graph to be transmitted for the maximum distortion suffered by the shortest paths between nodes of interest. This helps us design compression algorithms with attention to time performance of navigation tasks, for which paths planned on the compressed graph are not much longer compared to paths computed from the original graph containing fine-scale spatial information.

In contrast, closely related works are either restricted to trees or involve mixed-integer programming [33, 34]. In particular, the approach in [33] builds geometric abstractions on-the-fly without considering semantic or hierarchical information of the graph to be compressed. Other pruning strategies do not directly target path planning tasks and focus on computational efficiency of local task-planning algorithms [30]. Finally, most works tailored to real-time compression do not allow for hard communication constraints, either turning to soft constraints in the form of Lagrangian-like regularization [33], or focusing on computational aspects with feasibility requirements [30]. In particular, the work [30] proposes to prune the 3D Scene Graph to boost efficiency of a local task-planning routine, but it does not allow for sharp bounds on the size of the pruned graph, and further assumes that a specific task is known beforehand and only needs to be efficiently planned by the robot (*e.g.*, finding a way to grab and move specified objects).

The effectiveness of our algorithms is demonstrated through realistic simulation experiments. Our results show that the proposed compression methods meet hard communication constraints without excessively impacting efficiency of navigation tasks. For example, we show that navigation time on the compressed graph increases at most by 8% after compressing the full 3D Scene Graph to 1.6% of its original size.

Paper organization. In Section II, we present the motivating setup for navigation-oriented compression in the presence of communication constraints, and states 3D Scene Graph compression as an optimization problem which can be exactly solved via Integer Linear Programming (ILP). To circumvent

computational intractability of the ILP in practice, we design efficient algorithms that ensure to meet available communication resources while retaining spatial information useful for navigation. In particular, we leverage graph spanners to trade-off size of the compressed graph for distortion of shortest paths: mathematical background on spanners is provided in Section III, while explanation of our proposed algorithms is detailed in Section IV. In Section V, we test our approach with realistic simulation software for robotic exploration, and compare it to the compression approach in [33]. Final remarks and future research directions are given in Section VI.

II. NAVIGATION-ORIENTED SCENE GRAPH COMPRESSION

Motivating scenario. We consider a multi-robot team exploring an unknown environment. Each robot navigates to gather information and builds a 3D Scene Graph (DSG) $\mathcal{G} = (\mathcal{V}_{\mathcal{G}}, \mathcal{E}_{\mathcal{G}})$ that describes the portion of the environment explored so far [1–4]. As robots are scattered across a possibly large area, they exchange information to cooperatively gather information about the environment. In particular, a robot r_1 may query another robot r_2 to get information about the area explored by r_2 .¹

Navigation-oriented query. In this paper, we assume that the querying robot r_1 needs to reach one or more *target locations* $\mathcal{T} \subset \mathcal{V}_{\mathcal{G}}$ within the DSG $\mathcal{G} = (\mathcal{V}_{\mathcal{G}}, \mathcal{E}_{\mathcal{G}})$ of robot r_2 . Such locations, for instance, may be objects or points of interest (e.g., the building exits). Hence, r_2 shall transmit (a portion of) its local map such that r_1 can reach locations in \mathcal{T} from a set $\mathcal{S} \subset \mathcal{V}_{\mathcal{G}} \setminus \mathcal{T}$ of *source locations*. In practice, the latter may correspond to physical access points (e.g., doors) to the area explored by r_2 that are close to the current location of r_1 , and may be either communicated by r_1 or estimated by r_2 based on r_1 's position. In the following, we generically refer to sources and targets as *terminals*, which for the sake of this work are assumed to be *places* nodes in the DSG.

Communication constraints. Data sharing among robots occurs over a common wireless channel. Because of resource constraints of wireless communication, such as limited bit-rate and bandwidth, robot r_2 cannot transmit its entire DSG to robot r_1 . Specifically, we assume that robots can only send a small portion of their DSG each time they receive a share request.² Hence, queried robot r_2 needs to compress its DSG \mathcal{G} into a smaller graph $\mathcal{G}' = (\mathcal{V}_{\mathcal{G}'}, \mathcal{E}_{\mathcal{G}'})$, with at most B nodes (where B reflects the available communication budget), that complies with communication constraints while retaining information useful for robot r_1 to navigate between the terminal nodes.

Pruning 3D Scene Graphs. Assuming navigation-oriented queries, the relevant information reduces to nodes and edges enabling efficient paths robot r_1 can use to move from sources

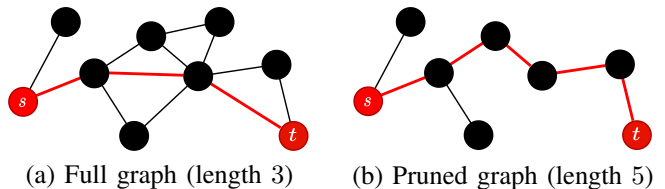


Figure 2: Distortion of shortest path from s to t (thick red).

to targets. Specifically, the collection of all shortest paths between each source $s \in \mathcal{S}$ and target $t \in \mathcal{T}$ represents the minimal information that can be transmitted to ensure that navigation by r_1 takes the minimum possible time, *i.e.*, the time a robot with complete knowledge of the map would take.

However, transmitting all nodes in the shortest paths may violate the communication constraint: this can happen with many terminals or if shortest paths have little overlap. Hence, heavier pruning of the DSG might be needed to make communication feasible. This means that information useful for path planning will be partially unavailable to the querying robot's planner. In other words, because the DSG \mathcal{G} cannot be fully communicated, the distance (length of a shortest path) between a pair of terminals in the transmitted graph \mathcal{G}' will be larger than the distance between those same terminals in the original DSG. A schematic example is provided in Fig. 2, where the length of the shortest path between nodes s and t increases from 3 to 5 after node and edge removal. For example, a robot may prune place nodes within a room, or share only the room node as a coarse representation of places. This requires less communication, but the querying robot r_1 , which receives a coarser map, will be forced to, *e.g.*, take a longer detour across a room, instead of traversing the original shortest path along a set of places nodes. Mathematically, this means $d_{\mathcal{G}'}(s, t) \geq d_{\mathcal{G}}(s, t)$ for any $s \in \mathcal{S}$ and for any $t \in \mathcal{T}$, where $d_{\mathcal{G}}(u, v)$ is the distance from node u to node v in \mathcal{G} .

Problem formulation. For the querying robot r_1 to navigate efficiently, it is desirable that the distance $d_{\mathcal{G}'}(s, t)$ between s and t in the transmitted graph \mathcal{G}' is not much larger than the distance in the original graph \mathcal{G} . Hence, the transmitting robot shall select nodes and edges in \mathcal{G} so as to minimize the *distortion*, or *stretch*, between shortest paths in the original and compressed graphs, while meeting the communication budget B . This can be cast into the following optimization problem:

$$\min_{\mathcal{G}' \subseteq \mathcal{G}} \beta \quad (1a)$$

$$\text{s.t. } d_{\mathcal{G}'}(s, t) \leq d_{\mathcal{G}}(s, t) + \beta W_{\max}^{\mathcal{G}}(s, t) \quad \forall (s, t) \in \mathcal{P}, \quad (1b)$$

$$|\mathcal{V}_{\mathcal{G}'}| \leq B, \quad (1c)$$

¹We assume robots talk with each other as soon as they get within communication range.

²Communication constraints can be practically intended as maximum transmission time T_{\max} : a robot first senses the channel and then, based on available communication resources, estimates the amount of information that can be sent in time T_{\max} . For example, assuming bit-rate r , specification of T_{\max} unambiguously defines the maximum amount of bits $b_{\max} = rT_{\max}$ to be sent, which is mapped to a DSG-related quantity (e.g., number of nodes).

where $W_{\max}^{\mathcal{G}}(u, v)$ denotes the maximum edge weight on a shortest path from u to v in \mathcal{G} , and $\mathcal{P} \subseteq \mathcal{S} \times \mathcal{T}$ is the set of source-target pairs considered for compression. Constraint (1c) ensures that the amount of transmitted information (number of nodes) meets the communication constraint, while constraint (1b) and cost (1a) encode minimization of the maximum distortion incurred by the shortest paths. The multiplicative coefficient $W_{\max}^{\mathcal{G}}(s, t)$ in (1b) is necessary to make the distortion

computation meaningful for weighted graphs.

Problem (1) can be solved exactly by means of integer linear programming (ILP), see Appendix A. However, the runtime complexity of ILP solvers is subject to combinatorial explosion, making this approach impractical for online operation. Hence, we propose greedy algorithms that require lighter-weight computation, based on *graph spanners*.

III. BACKGROUND: GRAPH SPANNERS

We ground our compression algorithm in the concept of *graph spanner* [17]. In words, a spanner is a compressed (*i.e.*, sparse) representation of a graph such that shortest paths between nodes are distorted at most by a user-defined stretch. Formally, a spanner $\mathcal{G}' = (\mathcal{V}, \mathcal{E}')$ of graph $\mathcal{G} = (\mathcal{V}, \mathcal{E})$ is a subgraph such that $\mathcal{E}' \subseteq \mathcal{E}$ and the following inequality holds for $u, v \in \mathcal{V}$,

$$d_{\mathcal{G}'}(u, v) \leq \alpha d_{\mathcal{G}}(u, v) + \beta W_{\max}^{\mathcal{G}}(u, v), \quad (2)$$

where $\alpha \geq 1$ and $\beta \geq 0$ are given constants. For generic α and β , \mathcal{G}' is called an (α, β) -spanner, whereas if β (resp. α) is equal to zero (resp. one) \mathcal{G}' is called α -*multiplicative* spanner (resp. β -*additive* or $+\beta$ spanner). Inequality (2) may hold for all nodes in \mathcal{G} or for a few pairs as in (1b): in the latter case, the resulting subgraph is referred to as a *pairwise spanner*.

Applications of spanners include navigation or packet routing in large graphs, whose size makes running path planning algorithms in the original graph computationally infeasible, [8, 37]. In this case, one can compute a spanner of the original graph and run planning algorithms on the spanner instead.

As one can see from (2), the characterization of spanners shares similarity with problem (1). Unfortunately, no method is known in the literature to build a spanner given a fixed node (or edge) budget, whereas algorithms usually enforce stretch (2) given input parameters α and β while attempting to minimize the total spanner edge-weight to obtain lightweight representations. The standard formulation of the graph spanner problem can be then written as follows [17, Problem 2],

$$\min_{\mathcal{E}_{\mathcal{G}'} \subseteq \mathcal{E}} \sum_{(i,j) \in \mathcal{E}_{\mathcal{G}'}} W^{\mathcal{G}}(i, j) \quad (3a)$$

$$\text{s.t.} \quad d_{\mathcal{G}'}(s, t) \leq \alpha d_{\mathcal{G}}(s, t) + \beta W_{\max}^{\mathcal{G}}(s, t), \quad (3b)$$

where $W^{\mathcal{G}}(i, j)$ is the weight of edge (i, j) and the objective function for unweighted graphs reduces to counting the number of edges. For multiplicative spanners this problem was quickly solved, with the classical work [38] proposing and analyzing a greedy algorithm which is known to be the best (in terms of spanner size) that runs in polynomial time. Additive and (α, β) -spanners are instead more complex to build, and many algorithms have been proposed in the literature: early efforts were devoted to unweighted graphs [39–42], while subsequent work has focused on the general weighted case [19, 43–45]. Other studies are concerned with distributed [46] and dynamical [47] methods, Euclidean graphs [48], and reachability preservation in digraphs [49], to mention a few.

To the best of our knowledge, the only paper to address the presence of an edge budget E_{\max} is [18]. However, the

algorithm proposed in [18] receives in input also parameters α and β , and checks feasibility of an (α, β) -spanner with at most E_{\max} edges. Furthermore, its runtime increases exponentially with E_{\max} , making it unsuitable for robotics applications.

A possible way to tackle the problem at hand is to iteratively build spanners with larger and larger distortion, until the budget is met. However, several issues can hamper such a strategy. First, running a spanner-building algorithm several times may be time-consuming. Second, while small-sized (*i.e.*, with $O(n^{1+\varepsilon(\alpha)})$ edges, for some $\varepsilon(\alpha) > 0$) multiplicative spanners can be built for any given constant coefficient $\alpha \geq 1$, few constant-distortion additive spanners are known for weighted graphs, with coefficient $\beta \in \{2, 4, 6\}$. Conversely, *polynomial* distortion $\beta = \beta(n)$ is needed to build additive spanners with near-linear size [41], thus the trade-off between spanner sparsity and path distortion is not easy to exploit.

An important point is that multiplicative and additive distortion may yield dramatic differences in paths induced by the spanner. In particular, multiplying path length by a constant factor in large graphs may be undesirable in practice: for example, if a navigation task nominally takes one hour, stretching it to two or three hours yields substantial performance degradation. Conversely, additive stretch is usually preferred because it provides a constant time overhead, which is why we used this kind of distortion in our problem formulation.

In the following, we illustrate a heuristic procedure that allows us to meet the budget constraint in (1c), runs in real time, and enforces a low distortion of shortest paths as measured by condition (1b).

IV. 3D SCENE GRAPH COMPRESSION ALGORITHMS

We propose D-Lite, a compression method for DSGs to meet communication constraints with attention to navigation efficiency. We design two versions of D-Lite, which leverage a spanner of the original full DSG (Section IV-B) and tackle the compression problem from opposite perspectives.

The first algorithm, BUD-Lite (Section IV-C), performs progressive bottom-up compression of the spanner computed during initialization, exploiting the DSG abstraction hierarchy. In contrast, the second algorithm, TOD-Lite, (Section IV-D), works top-down expanding nodes with the spanner as a target.

A. The Role of the 3D Scene Graph Hierarchy

Ideally, navigation-oriented compression of a DSG would require searching among all possible subgraphs of \mathcal{G} to find one that minimally stretches paths between terminals. Such a search is prone to combinatorial blow-up and is thus impractical.

Here, we seek a greedy procedure that removes nodes and edges in \mathcal{G} while trying to limit the incurred path stretch. This goal is subject to a nontrivial trade-off. On the one hand, to ensure low stretch (*i.e.*, retain navigation performance), it is desirable to parse one or a few nodes at each iteration so as to introduce extra distortion in a controlled way. On the other hand, parsing too few nodes at each time induces a large number of total iterations, and is computationally expensive for online

operation. Hence, an effective algorithm should effectively choose the size of node batch to be greedily compressed at each iteration to strike a balance between compression quality and runtime.

Towards this goal, we crucially exploit the *hierarchical structure* of the DSG. The latter allows us to see a node n_ℓ in layer ℓ of the DSG \mathcal{G} as a “compressed” representation of its children nodes $\mathcal{V}_{\mathcal{G}}(n_\ell)$ in layer $\ell + 1$: hence, transmitting n_ℓ rather than $\mathcal{V}_{\mathcal{G}}(n_\ell)$ saves communication while also conveying partial spatial information about $\mathcal{V}_{\mathcal{G}}(n_\ell)$. For example, assume that $\mathcal{V}_{\mathcal{G}}(n_\ell)$ represents a set of places within a room and n_ℓ is the corresponding room node. A robot that needs to reach a specific location $t \in \mathcal{V}_{\mathcal{G}}(n_\ell)$ (e.g., the exit door) in that room, can be provided a sequence of places to reach that location. Alternatively, the robot can be given the room node n_ℓ , and it can explore the room to find the target location. This extra exploration (corresponding to additional path stretch in the compressed DSG) degrades navigation performance, however it allows for great compression useful to meet the communication constraint. Mathematically, the navigation time for local exploration (e.g., to reach a place from the room centroid) is encoded by weights of cross-layer edges. The same holds for edges connecting nodes in the same layer with no direct path (e.g., to move from a room to another room without knowledge of intermediate place nodes). Details about the calculation of such weights, which we assume a robot with the full DSG can estimate, are provided in Appendix B.

The discussion above suggests a simple approach to compress the DSG: a greedy procedure can be devised so that nodes in upper layer ℓ can be progressively selected so as to replace their children nodes in layer $\ell - 1$. Every time we “abstract away” places nodes for more abstract nodes (e.g., rooms, buildings) the length of the paths passing through those nodes will increase. Therefore, we can opportunistically select places nodes that entail a small stretch in the paths between the terminal nodes. In alternative, we can start with a minimal representation (e.g., one including only rooms and buildings) and iteratively expand it to reduce the stretch of the paths between terminal nodes. We present these two greedy strategies below, and initialize both procedures by computing a spanner of the given DSG, as described next.

B. Building a DSG Spanner

Both proposed algorithms build a spanner of the DSG during initialization. A detailed description of how each procedure uses this spanner is deferred to Sections IV-C and IV-D.

Algorithm 1 describes how to build a spanner of the DSG that enforces a user-defined maximum additive stretch for distances between specified terminal pairs in \mathcal{P} . We adapt our algorithm from [19, Section 5]. Specifically, the procedure [19] can trade spanner size for stretch according to input parameters, building a $+cn^{\frac{1-\epsilon}{2}}\alpha W_{\max}^{\mathcal{G}}$ spanner of size $O(n^{1+\epsilon})$.³ That algorithm is intended for generic spanners (not pairwise), hence we adapt it to our scope by retaining only nodes and

Algorithm 1 Build spanner

Input: DSG \mathcal{G} , terminal pairs \mathcal{P} , user parameters $\epsilon > 0, p \in [0, 1], \alpha > 2, c > 0$.

Output: DSG spanner \mathcal{G}' .

```

1:  $\mathcal{G}'_1 \leftarrow n^\epsilon$ -light initialization of  $\mathcal{G}$ ;
2:  $\mathcal{G}'_2 \leftarrow$  random sample of cross-layer edges of  $\mathcal{G}$  w.p.  $p$ ;
3:  $\mathcal{G}'_3 \leftarrow \alpha$ -multiplicative spanner of  $\mathcal{G}$ ;
4:  $\mathcal{G}'' \leftarrow \mathcal{G}'_1 \cup \mathcal{G}'_2 \cup \mathcal{G}'_3$ ; // to compute paths
5:  $\mathcal{G}' \leftarrow \mathcal{P}$ ;
6: for each  $(s, t) \in \mathcal{P}$  do // sorted by  $W_{\max}^{\mathcal{G}}(s, t)$ 
7:   if  $d_{\mathcal{G}''}(s, t) > d_{\mathcal{G}}(s, t) + cn^{\frac{1-\epsilon}{2}}\alpha W_{\max}^{\mathcal{G}}(s, t)$  then
8:      $\mathcal{G}'' \leftarrow \mathcal{G}'' \cup P_{\mathcal{G}}(s, t)$ ;
9:      $\mathcal{G}' \leftarrow \mathcal{G}' \cup P_{\mathcal{G}}(s, t)$ ;
10:  else
11:     $\mathcal{G}' \leftarrow \mathcal{G}' \cup P_{\mathcal{G}''}(s, t)$ ;
12:  end if
13: end for
14: return  $\mathcal{G}'$ .
```

edges needed to connect terminal pairs in \mathcal{P} , and deleting all others. Algorithm 1 is composed of two sequential stages: an initialization phase that builds a temporary spanner \mathcal{G}'' with a small number of edges that attempts to keep low initial path distortions, and a “buying” phase where edges are added to meet the stretch constraint. The initialization selects edges in three ways: performing a d -light initialization [44, Section 2] with appropriate d (Line 1), which in words ensures that each node has some initial neighbors; randomly picking cross-layer edges to exploit the DSG hierarchy (Line 2); adding a greedy multiplicative spanner [38, Section 2] to reduce large path distortions (Line 3). Then, for each pair (s, t) the shortest path $P_{\mathcal{G}''}(s, t)$ from source s to target t in the temporary spanner \mathcal{G}'' is considered (in suitable order): in case the stretch in \mathcal{G}'' exceeds the constraint, edges and nodes from a shortest path in the original graph \mathcal{G} are added to both \mathcal{G}'' and the final spanner \mathcal{G}' (Lines 8–9), otherwise, the shortest path in \mathcal{G}'' is directly added to the final spanner \mathcal{G}' (Line 11). We refer to this subroutine as `build_spanner`.

Before diving into the core of our compression algorithms, it is worth reinforcing the motivation to use graph spanners. Algorithm 1 outputs a spanner with given maximal stretch of shortest paths, but does not guarantee that the produced spanner matches the desired node budget B . As noted in Section III, we cannot straightly apply a state-of-the-art spanner construction because no real-time algorithm in the literature addresses the presence of an exact budget. However, building a spanner greatly reduces the graph to be compressed up front, retaining only nodes and edges which both are relevant for navigation and sharply enhance efficiency of our proposed compression strategies. Moreover, even though path distortion may be increased to satisfy communication requirements, the user-defined stretch guaranteed by the spanner algorithm allows us to start from a maximum desired distortion: hence, if the latter is chosen loose enough, we may expect that the spanner output by Algorithm 1 is already somewhat close to the

³Parameter α might depend on n , e.g., the authors in [19] use $\alpha(n) = \log n$.

communication constraint, so that additional distortion will not be very high. In particular, the spanner construction leverages overlapping portions of paths to select a handful of key edges and nodes, whereas other navigation-efficient constructions, such as the collection of all shortest paths, do not exploit the graph structure to enhance compression. Furthermore, there are no tight bounds for the size of shortest paths, hence one cannot predict how much paths will be stretched in order to meet the communication budget.

C. BUD-Lite: a Bottom-Up Compression Algorithm

The key idea behind our first algorithm (BUD-Lite, short for Bottom-Up D-Lite) is to iteratively *compress* the DSG spanner produced by Algorithm 1 according to the discussion in Section IV-A. The mechanism is simple: we progressively replace batches of nodes with their parents to reduce size, while attempting to keep the stretch suffered by shortest paths between terminals low. To enhance compression granularity, we consider one terminal pair (s, t) at a time and compress a stretch of places nodes along the shortest path, replacing them with an abstract representation such as room or building node.

To gain some intuition, consider Fig. 3, which illustrates three consecutive iterations of BUD-Lite on a toy DSG. Dashed edges and light-colored nodes are part of the full DSG \mathcal{G} , and potential candidates to be added to the compressed DSG \mathcal{G}' . Conversely, the latter is marked with solid lines and darker colors. The initial spanner (top left) contains all place nodes, thus retains precise spatial information but does not meet the communication budget. The first iteration of BUD-Lite parses the shortest path from s to t_1 and abstracts away places nodes associated with the first encountered room node (top right). Specifically, places nodes P_3 and P_4 are removed and replaced with room node R_2 , which is an abstract representation of those places. R_1 is not considered because it yields no budget reduction as compared to keeping node P_1 . P_2 is not removed at this point because it lies also on the shortest path connecting pair (s, t_2) . Node P_2 is indeed removed at the second iteration, when the shortest path from s to t_2 is entirely parsed and shortcut via place node P_1 and room node R_2 (bottom right). The final iteration parses the last portion of the path connecting (s, t_1) , and shortcuts the remaining places nodes P_5 and P_6 under rooms nodes R_2 and R_3 (bottom left). An example on an actual DSG build from synthetic data is shown in Fig. 4, where the room node is used to abstract several places nodes. More results on DSGs from synthetic navigation data are provided in Appendix C.

We more formally introduce the compression procedure in Algorithm 2. Algorithm 2 initially sets the compressed graph as the DSG spanner \mathcal{G}' output by Algorithm 1 (Line 1). The external loop at Line 6 parses each layer ℓ of \mathcal{G}' , starting the bottom layer ($\ell = 0$) and going up. At each iteration of the inner loop at Line 7, the algorithm checks if the shortest path $P_{\mathcal{G}'}(s, t)$ connecting terminals s and t contains a stretch of nodes in layer ℓ with the same parent node $n_{\ell+1}$, which is denoted by $\mathcal{V}_{\mathcal{G}}(n_{\ell+1})$ (Line 8): if such a stretch is found, all nodes in $\mathcal{V}_{\mathcal{G}}(n_{\ell+1})$ are removed from

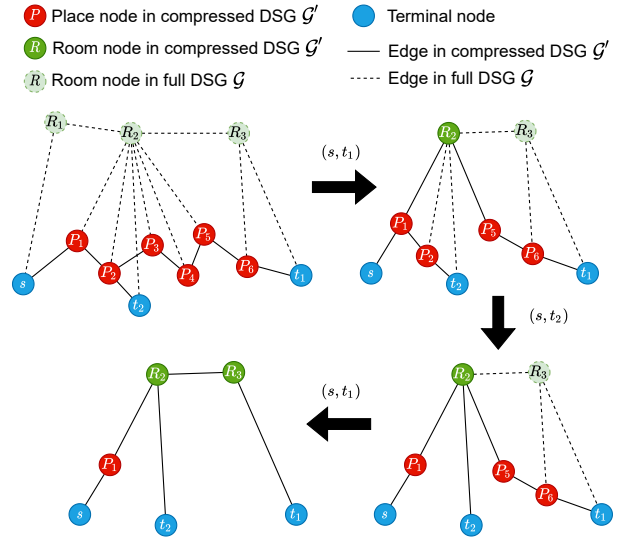


Figure 3: Illustration of the BUD-Lite procedure with source s and targets t_1, t_2 . At each iteration, places nodes in a shortest path between terminals are replaced by a room node. Nodes are removed when none of the terminal pairs (s, t_1) and (s, t_2) connects through them. Note that the final graph cannot be further pruned without disconnecting terminals.

$P_{\mathcal{G}'}(s, t)$ and replaced (*compressed*) with their parent $n_{\ell+1}$ (Line 9).⁴ Importantly, such *compression* in the graph causes a corresponding *stretch* of the actual path followed by the robot, the amount of which depends on both the interested layer ℓ and the number of compressed nodes, in light of what we discussed in Section IV-A. Nevertheless, the nested structure looping over layers externally (Line 6) and over paths internally (Line 7) introduces just one upper-layer abstraction at a time for each path (the layer ℓ is fixed in loop Line 7), and hence allows us to stretch distances in a balanced fashion, so that all paths are expected to suffer comparable distortion eventually. For example, if paths are made of places nodes, the first iteration of the inner loop compresses only one room for each path, so that at no point during the compression procedure a path is overly compressed with respect to other paths (*i.e.*, it is not possible that a path is entirely abstracted to room nodes while another is kept with all places nodes). In general, this allows fine-scale spatial information to be retained as long as possible, and coarser layers (*e.g.*, buildings) to be used only after finer layers (*e.g.*, rooms) have been fully exploited for all paths (*i.e.*, building nodes can be used only if all paths contain room nodes and no places nodes). To ensure paths remain feasible, we use a data structure \mathcal{D} to track which paths are using nodes in \mathcal{G}' (Line 3): only when a node is traversed by no path (Line 13), it is removed from the graph.

D. TOD-Lite: a Top-Down Expansion Algorithm

Symmetrically to the bottom-up approach of Algorithm 2, the idea behind TOD-Lite (short for Top-down D-Lite) is to exploit

⁴For consistency of navigation, we do not compress terminal nodes in our implementation, but this can be changed to meet communication constraints.

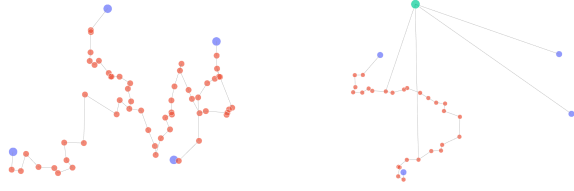


Figure 4: Initial (left) and final DSG spanners (right). Terminal nodes are in blue, place nodes in red, room node in green.

Algorithm 2 BUD-Lite

Input: DSG \mathcal{G} , terminal pairs \mathcal{P} , communication budget B .
Output: Compressed DSG \mathcal{G}' .

- 1: $\mathcal{G}' \leftarrow \text{build_spanner}(\mathcal{G}, \mathcal{P});$ // initialization
- 2: **for each** node $n \in \mathcal{V}_{\mathcal{G}'}$ **do** // track node usage
- 3: $\mathcal{D}[n] \leftarrow$ subset of terminals pairs whose shortest path in \mathcal{G}' passes through n ;
- 4: **end for**
- 5: **while** $|\mathcal{V}_{\mathcal{G}'}| > B$ **do**
- 6: **for each** layer $\ell = 0, \dots, L - 1$ **do**
- 7: **for each** $(s, t) \in \mathcal{P}$ **do** // parse path from s to t
- 8: **if** \exists stretch of nodes $\mathcal{V}_{\mathcal{G}}(n_{\ell+1}) \subseteq P_{\mathcal{G}'}(s, t)$ **then**
- 9: replace $\mathcal{V}_{\mathcal{G}}(n_{\ell+1})$ with $n_{\ell+1}$ in $P_{\mathcal{G}'}(s, t)$;
- 10: $\mathcal{D}[n_{\ell+1}] \leftarrow \mathcal{D}[n_{\ell+1}] \cup (s, t)$;
- 11: **for each** node $n'_\ell \in \mathcal{V}_{\mathcal{G}}(n_{\ell+1})$ **do**
- 12: $\mathcal{D}[n'_\ell] \leftarrow \mathcal{D}[n'_\ell] \setminus (s, t)$;
- 13: **if** $\mathcal{D}[n'_\ell] = \emptyset$ **then** // if unused,
- 14: $\mathcal{G}' \leftarrow \mathcal{G}' \setminus \{n'_\ell\}$; // delete n'_ℓ
- 15: **end if**
- 16: **end for**
- 17: **end if**
- 18: **end for**
- 19: **end while**
- 20: **return** \mathcal{G}' .

the DSG hierarchy by expanding node children to iteratively increase spatial granularity of the compressed graph (Fig. 5).

During initialization, Algorithm 3 first builds a spanner $\mathcal{G}'_{\text{target}}$ of the DSG with Algorithm 1, which is used as target for the final compressed graph \mathcal{G}' (Line 1). Then, it populates a “hierarchical spanner” \mathcal{H} (Line 2): this is simply a graph obtained from the original DSG \mathcal{G} by keeping the spanner $\mathcal{G}'_{\text{target}}$ plus nodes and edges encountered by starting from $\mathcal{G}'_{\text{target}}$ and going up the DSG hierarchy all the way to the top layer. Elements unrelated to the ancestors of $\mathcal{G}'_{\text{target}}$ are removed. For example, if $\mathcal{G}'_{\text{target}}$ is made of place nodes, \mathcal{H} includes $\mathcal{G}'_{\text{target}}$, the room nodes associated with those places (together with edges among them), and possibly nodes above in the hierarchy, e.g., the buildings collecting those rooms. Graph \mathcal{H} is used to expand nodes from coarser to finer layers, as explained next. To define an expansion priority for nodes in the same layer, a data structure \mathcal{D} stores how many paths pass through each node in the graph, including both original paths in the target spanner (Line 4) and path abstractions in upper layers (Line 8): for example, the priority of a room node R is given by the

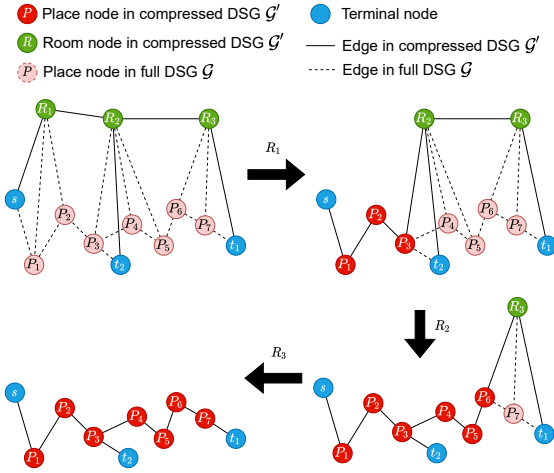


Figure 5: Illustration of the TOD-Lite expansion procedure with one source s and two targets t_1 and t_2 . At each iteration, a room node is expanded and replaced with its children place nodes. Adjacent place nodes are possibly added to ensure connectivity between terminals (e.g., P_3 at the first iteration).

number of paths actually passing through R in $\mathcal{G}'_{\text{target}}$ and of paths traversing places nodes associated with R .

The main phase is an iterative top-down expansion through the hierarchical spanner \mathcal{H} . The output spanner \mathcal{G}' is initialized with terminal nodes (Line 11) and cross-layer connections (Line 12) to ensure minimum-cardinality paths, hence small communication cost.⁵ Then, starting from the top layer L and going down one layer at a time (Line 17), each node in \mathcal{G}' is *expanded* if such operation does not exceed the budget (Line 19), until no expansion is possible (Line 25). In particular, if a node n_ℓ belonging to layer ℓ of \mathcal{G}' has a set of children $\mathcal{V}_{\mathcal{H}}(n_\ell)$ in the hierarchical spanner \mathcal{H} , then Line 20 removes the node n_ℓ and Line 21 adds to \mathcal{G}' nodes in $\mathcal{V}_{\mathcal{H}}(n_\ell)$ their incident edges. This mechanism is illustrated in Fig. 5, where room nodes R_1 , R_2 , and R_3 are progressively replaced with their respective children nodes. The starting condition (top left) ensures connectivity between terminals under low budget, but conveys little information useful for navigation because of the coarse spatial abstractions provided by rooms nodes.

Importantly, expanding nodes gradually restores the geometric granularity of the output spanner, because a spatially coarse representation (e.g., room node) is replaced by a group of nodes and edges carrying finer spatial resolution (e.g., in the places layer). Such expansion of course comes at the price of heavier communication burden. Nonetheless, using the hierarchical spanner allows us to narrow the expansion procedure to a small set of navigation-relevant nodes, both saving runtime and helping us meet communication constraints.

Note that, with enough communication resources, this procedure would output exactly the target spanner $\mathcal{G}'_{\text{target}}$. Under limited budget, some nodes in $\mathcal{G}'_{\text{target}}$ cannot be expanded, e.g., a room may be used as a coarse representation of its places.

⁵Again, we assume that a minimal communication budget is always available to transmit at least such minimum-cost paths between terminals.

Algorithm 3 TOD-Lite

Input: DSG \mathcal{G} , terminal pairs \mathcal{P} , communication budget B .

Output: Compressed DSG \mathcal{G}' .

```
1:  $\mathcal{G}'_{\text{target}} \leftarrow \text{build\_spanner}(\mathcal{G}, \mathcal{P});$ 
2:  $\mathcal{H} \leftarrow \text{hierarchical spanner from } \mathcal{G}'_{\text{target}};$ 
3: for each node  $n$  do // for expansion priority
4:    $\mathcal{D}[n] \leftarrow$  number of terminals pairs whose shortest path
   in  $\mathcal{G}'_{\text{target}}$  passes through  $n$ ;
5: end for
6: for each layer  $\ell = 1, \dots, L$  do
7:   for each node  $n_\ell$  do
8:      $\mathcal{D}[n_\ell] \leftarrow \mathcal{D}[n_\ell] \cup \bigcup_{n'_{\ell-1} \in \mathcal{V}_{\mathcal{G}}(n_\ell)} \mathcal{D}[n'_{\ell-1}];$ 
9:   end for
10: end for
11:  $\mathcal{G}' \leftarrow \mathcal{P};$  // add terminals
12: for each  $(s, t) \in \mathcal{P}$  do // add cheapest path from  $s$  to  $t$ 
13:    $a \leftarrow$  lowest common ancestor of  $s$  and  $t$  in  $\mathcal{H}$ ;
14:    $\mathcal{G}' \leftarrow \mathcal{G}' \cup \{a\};$ 
15:   connect  $s$  and  $t$  with  $a$  in  $\mathcal{G}'$ ;
16: end for
17: for each layer  $\ell = L, \dots, 1$  do
18:   for each node  $n_\ell$  do // sorted by  $\mathcal{D}[n_\ell]$ 
19:     if can expand  $n_\ell$  without exceeding  $B$  then
20:        $\mathcal{G}' \leftarrow \mathcal{G}' \setminus \{n_\ell\};$ 
21:        $\mathcal{G}' \leftarrow \mathcal{G}' \cup \mathcal{V}_{\mathcal{H}}(n_\ell) \cup \mathcal{E}_{\mathcal{H}}(\mathcal{V}_{\mathcal{H}}(n_\ell));$ 
22:     end if
23:   end for
24:   if no node  $n_\ell$  has been expanded then
25:     break;
26:   end if
27: end for
28: return  $\mathcal{G}'$ .
```

Experimental results of TOD-Lite are provided in Appendix C.

Comparison with [33]. Our node-expansion procedure resembles the approach used in [33]. However, there are fundamental differences between these two methodologies. First, we expand nodes along a preexisting semantic hierarchical structure (the 3D Scene Graph), while the hierarchy in [33] simply emerges from the regular geometry of the environment (such as a grid map in [33, 35]), without awareness of semantics or physical quantities such as navigation time to move through coarse- and fine-scale maps. Second, our expansion leverages a target spanner computed up front and is guided by the navigation task, in particular by the stretch incurred by the shortest paths, while nodes in [33] are expanded based on an information-theoretic cost to be defined by suitable probability distributions whose support and density function change with expansions but are initially defined on the full graph to be compressed. More details about the algorithm in [33] are given in Section V.

V. EXPERIMENTS

This section shows that the compressed DSG using our method is able to retain information for efficient navigation while

meeting the communication budget constraint. We also show that the compression can be done in real-time.

A. Experimental Setup

Besides benchmarking D-Lite against the solution to (1) (label: “Optimum”) found via integer linear programming (ILP), we also adapt the information theoretic approach proposed in [33] as a baseline for comparison (label: “IB”), as discussed below.

Q-Tree search adaptation. The compression approach proposed in [33] is based on the Information Bottleneck (IB) framework [50]. The goal of the compression approach is to find a compact representation T of a given random variable X by solving a relaxed version of the IB problem,

$$\min_{p(T|X)} I(T; X) - \beta \cdot I(T; Y), \quad (4)$$

where $I(T; X)$ is the mutual information between T and X and $I(T; Y)$ represents the information that T retains about a third variable Y which encodes relevant information about X . Parameter β can be seen as a knob to trade-off amount of relevant information retained in T for compression rate.

To adapt this approach to navigation-oriented DSG compression, we define a uniform distribution $p(x)$ over the places nodes; next, we associate Y with shortest paths between terminals: if place x_i is on the shortest path y_j , then $p(y_j|x_i) = 1$, and $p(y_j|x_i) = 0$ otherwise. From the places layer, we build X by propagating $p(x)$ and $p(y|x)$ to rooms and buildings layers by a weighted sum as shown in [33]. We manually add the terminal nodes to the result if they are not automatically added by the algorithm, and in view of (1) we use the number of nodes as stopping condition in addition to the one in [33].

Simulator. We showcase the online operation of D-Lite in the uHumans2 simulator [51]. In the Office environment of the uHumans2 simulator (Fig. 1), we devised 4 scenarios ranging from short, medium, to long in terms of the distance between the navigation goal and the starting position of the robot.

The queried robot r_2 sending the compressed DSG has no exact knowledge of the location of the querying robot r_1 , and is only given some potential locations. The places closest to these source locations along with the place closest to the navigation goal are chosen as terminals for D-Lite. In the short and medium sequences, r_1 gets two putative source locations, hence three total terminals. In the two long sequences, r_1 gets three putative source locations, hence four total terminals. For all sequences, we chose the communication budget to be 60 nodes, which is about 1.6% of the full DSG.

Upon receiving the compressed DSG, robot r_1 finds the place node s closest to its current location, then computes the shortest path from s to the place node t that represents the navigation goal. Robot r_1 treats the nodes along the shortest path as waypoints to navigate to the goal. We combine waypoint following with the use of the ROS navigation stack for local obstacle avoidance: the latter is needed where free-space locations are not available to r_1 (*i.e.*, when places nodes are not communicated for a portion of the map).

Table I: Summary of results. Arrows indicate that lower is better. The table reports mean and deviation across three runs.

	Full	Optimum	IB	BUD-Lite	TOD-Lite	
short	Comp(s) ↓	0 ± 0	247 ± 0	1 ± 0	3 ± 0	3 ± 0
	Nom(s) ↓	11 ± 0	11 ± 0	43 ± 0	11 ± 0	11 ± 0
	Mis(s) ↓	64 ± 8	56 ± 5	115 ± 16	62 ± 2	59 ± 3
	Size(≤60)	3814 ± 0	51 ± 0	60 ± 0	49 ± 0	49 ± 0
medium	Comp(s) ↓	0 ± 0	294 ± 1	1 ± 0	3 ± 0	3 ± 0
	Nom(s) ↓	18 ± 0	18 ± 0	42 ± 0	18 ± 0	29 ± 0
	Mis(s) ↓	87 ± 7	77 ± 2	92 ± 22	85 ± 8	144 ± 20
	Size(≤60)	3814 ± 0	56 ± 0	60 ± 0	48 ± 0	58 ± 0
long1	Comp(s) ↓	0 ± 0	-	2 ± 0	3 ± 0	3 ± 0
	Nom(s) ↓	27 ± 0	-	∞	31 ± 0	39 ± 0
	Mis(s) ↓	134 ± 5	-	∞	167 ± 18	273 ± 22
	Size(≤60)	3814 ± 0	-	60 ± 0	58 ± 0	20 ± 0
long2	Comp(s) ↓	0 ± 0	-	2 ± 0	3 ± 0	3 ± 0
	Nom(s) ↓	32 ± 0	-	36 ± 0	33 ± 0	34 ± 0
	Mis(s) ↓	150 ± 6	-	218 ± 20	164 ± 30	291 ± 39
	Size(≤60)	3814 ± 0	-	60 ± 0	60 ± 0	9 ± 0

B. Results and Discussion

The results on the four scenarios are documented in Table I. We show the compression time (label: “Comp”), the nominal (label: “Nom”, computed from the compressed DSG) and simulated (label: “Mis”, computed as the actual time r_1 takes to reach its destination in the simulator) mission times, and the size of the compressed DSG, all averaged across three separate runs.⁶ The two best results for each row are highlighted in bold.

The combinatorial nature of the problem makes the ILP solver impractical in robotics applications: for the two long runs, the calculation of Optimum did not finish within an hour.

In general, in all four sequences, robot r_1 is able to effectively reach the navigation goal using the compressed DSG output by D-Lite. The simulated mission time is at times faster on the compressed graph compared to the full DSG due to the former having to visit fewer waypoints: a sparser list of node waypoints in a less cluttered space could actually yield faster navigation. The different performance of BUD-Lite (bottom-up compression) and TOD-Lite (top-down expansion) is due to the different abstraction mechanisms, whereby the path-wise node compression in the former enjoys finer granularity and usually yields better performance. Note that discrepancies between nominal and simulated mission times are due to local navigation, whose exploration time is difficult to estimate *a posteriori*, but may be more reliably estimated by the robot while building the DSG online. Notably, our approaches always outperform IB in terms of both nominal and simulated mission time. Specifically, the compressed DSG generated by BUD-Lite yields navigation time that is within a minute of the optimal navigation time achieved by planning on the full DSG.

⁶The nominal mission time is computed by projecting the waypoints found by r_1 (in the compressed DSG) onto the full DSG, calculating the total path length of traversing through those on the full DSG, and dividing by the maximum velocity of the agent. In other words, it is the theoretical navigation time on the original DSG and quantifies quality of the compression. Note that we do not directly use the compressed DSG to estimate the nominal time because the cross-layer edge weights would be different and likely smaller in value compared to those calculated on the full DSG, see Appendix B.

VI. CONCLUSIONS

Motivated by the goal of enabling efficient information sharing for robots that collaboratively explore an unknown environment, we have proposed algorithms to suitably compress 3D Scene Graphs built and transmitted by robots during exploration, for the case when resource constraints of a shared communication channel make lossless transmission infeasible. Our algorithms can accommodate the presence of a sharp budget on the size of the transmitted map, run in real time, and perform graph compression with attention to the performance on specified navigation tasks. Simulated experiments carried out with a realistic simulator show that our approach is able to meet communication constraints while providing satisfactory performance of navigation tasks planned on the compressed DSG.

The proposed approach opens several interesting avenues for future work. In fact, 3D Scene Graphs are recently developed tools, and their use in multi-robot cooperation and collaboration is still relatively unexplored. For example, it is interesting to adapt our compression algorithms to data collection in dynamic environments —as the ones considered in [51]— that induce time-varying graphs. Also, extension of compression techniques to various and more general tasks should be addressed. Finally, validation of the proposed algorithms on real robots is desired to test their impact in the real world.

REFERENCES

- [1] A. Rosinol, A. Gupta, M. Abate, J. Shi, and L. Carlone, “3D dynamic scene graphs: Actionable spatial perception with places, objects, and humans,” in *Robotics: Science and Systems (RSS)*, 2020, (pdf), (media), (video). [Online]. Available: <http://news.mit.edu/2020/robots-spatial-perception-0715>
- [2] N. Hughes, Y. Chang, and L. Carlone, “Hydra: a real-time spatial perception engine for 3D scene graph construction and optimization,” in *Robotics: Science and Systems (RSS)*, 2022, (pdf).
- [3] I. Armeni, Z. He, J. Gwak, A. Zamir, M. Fischer, J. Malik, and S. Savarese, “3D scene graph: A structure for unified semantics, 3D space, and camera,” in *Intl. Conf. on Computer Vision (ICCV)*, 2019, pp. 5664–5673.
- [4] S. Wu, J. Wald, K. Tateno, N. Navab, and F. Tombari, “SceneGraphFusion: Incremental 3D scene graph prediction from RGB-D sequences,” in *IEEE Conf. on Computer Vision and Pattern Recognition (CVPR)*, 2021.
- [5] U. Kim, J. Park, T. Song, and J. Kim, “3-D scene graph: A sparse and semantic representation of physical environments for intelligent agents,” *IEEE Trans. Cybern.*, vol. PP, pp. 1–13, Aug. 2019.
- [6] R. Talak, S. Hu, L. Peng, and L. Carlone, “Neural trees for learning on graphs,” in *Conf. on Neural Information Processing Systems (NeurIPS)*, 2021, (pdf).
- [7] A. Becker, P. N. Klein, and D. Saulpic, “A Quasi-Polynomial-Time Approximation Scheme for Vehicle Routing on Planar and Bounded-Genus Graphs,” in *Proc. of the Annual European Symp. on Algorithms (ESA)*, vol. 87, 2017, pp. 12:1–12:15.
- [8] A. Dobson and K. E. Bekris, “Sparse roadmap spanners for asymptotically near-optimal motion planning,” *Intl. J. of Robotics Research*, vol. 33, no. 1, pp. 18–47, Jan. 2014.
- [9] A. C. Gilbert, T. Labs-Research, P. Avenue, F. Park, and K. Levchenko, “Compressing Network Graphs,” *Proc. of the LinkKDD workshop at the ACM Conference on KDD*, vol. 124, p. 10, 2004.
- [10] R. L. de Queiroz and P. A. Chou, “Compression of 3D Point Clouds Using a Region-Adaptive Hierarchical Transform,” *IEEE Trans. on Image Processing*, vol. 25, no. 8, pp. 3947–3956, Aug. 2016.
- [11] X. Sun, H. Ma, Y. Sun, and M. Liu, “A novel point cloud compression algorithm based on clustering,” *IEEE Robotics and Automation Letters*, vol. 4, no. 2, pp. 2132–2139, 2019.
- [12] D. Thanou, P. A. Chou, and P. Frossard, “Graph-based compression of dynamic 3d point cloud sequences,” *IEEE Transactions on Image Processing*, vol. 25, no. 4, pp. 1765–1778, 2016.

- [13] S. Raghavan and H. Garcia-Molina, "Representing Web graphs," in *Proc. International Conference on Data Engineering (Cat. No.03CH37405)*, Mar. 2003, pp. 405–416.
- [14] C. Chekuri, T. Rukkanchanunt, and C. Xu, "On Element-Connectivity Preserving Graph Simplification," in *Algorithms - ESA 2015*, Berlin, Heidelberg, 2015, pp. 313–324.
- [15] P. Harish, P. J. Narayanan, V. Vineet, and S. Patidar, "Chapter 7 - Fast Minimum Spanning Tree Computation," in *GPU Computing Gems Jade Edition*, ser. Applications of GPU Computing Series, Jan. 2012, pp. 77–88.
- [16] K. Mehlhorn, "A faster approximation algorithm for the Steiner problem in graphs," *Information Processing Letters*, vol. 27, no. 3, pp. 125–128, Mar. 1988.
- [17] R. Ahmed, G. Bodwin, F. D. Sahneh, K. Hamm, M. J. L. Jebelli, S. Kobourov, and R. Spence, "Graph spanners: A tutorial review," *Computer Science Review*, vol. 37, p. 100253, Aug. 2020.
- [18] Y. Kobayashi, "An FPT Algorithm for Minimum Additive Spanner Problem," in *International Symposium on Theoretical Aspects of Computer Science (STACS)*, vol. 154, 2020, pp. 11:1–11:16.
- [19] M. Elkin, Y. Gitlitz, and O. Neiman, "Improved weighted additive spanners," *Distrib. Comput.*, Aug. 2022.
- [20] G. Bodwin, "On the Structure of Unique Shortest Paths in Graphs," in *Proc. of the Annual ACM-SIAM Symp. on Discrete Algorithms (SODA)*, Jan. 2019, pp. 2071–2089.
- [21] M. Elkin and O. Neiman, "Efficient Algorithms for Constructing Very Sparse Spanners and Emulators," *ACM Trans. Algorithms*, vol. 15, no. 1, pp. 4:1–4:29, Nov. 2018.
- [22] U. Kang and C. Faloutsos, "Beyond 'Caveman Communities': Hubs and Spokes for Graph Compression and Mining," in *Proc. of the IEEE International Conference on Data Mining*, Dec. 2011, pp. 300–309.
- [23] M. Besta and T. Hoefler, "Survey and Taxonomy of Lossless Graph Compression and Space-Efficient Graph Representations," *arXiv:1806.01799 [cs, math]*, Apr. 2019.
- [24] A. Borici and A. Thomo, "Semantic Graph Compression with Hypergraphs," in *IEEE International Conference on Advanced Information Networking and Applications*, Victoria, BC, Canada, May 2014, pp. 1097–1104.
- [25] J.-G. Young, G. Petri, and T. P. Peixoto, "Hypergraph reconstruction from network data," *Commun. Phys.*, vol. 4, no. 1, p. 135, Dec. 2021.
- [26] G. Karypis and V. Kumar, "Multilevel k-Way Hypergraph Partitioning," in *Design Automation Conference*, Jun. 1999, pp. 343–348.
- [27] K. Devine, E. Boman, R. Heaphy, R. Bisseling, and U. Catalyurek, "Parallel hypergraph partitioning for scientific computing," in *Proc. of the IEEE International Parallel & Distributed Processing Symposium*, 2006, p. 10 pp.
- [28] S. Zhang, Z. Ding, and S. Cui, "Introducing Hypergraph Signal Processing: Theoretical Foundation and Practical Applications," *IEEE Internet Things J.*, vol. 7, no. 1, pp. 639–660, Jan. 2020.
- [29] T. Silver, R. Chitnis, A. Curtis, J. B. Tenenbaum, T. Lozano-Pérez, and L. P. Kaelbling, "Planning with Learned Object Importance in Large Problem Instances using Graph Neural Networks," *Proc. of the AAAI Conference on Artificial Intelligence*, vol. 35, no. 13, pp. 11 962–11 971, May 2021.
- [30] C. Agia, K. M. Jatavallabhula, M. Khodeir, O. Miksik, V. Vineet, M. Mukadam, L. Paull, and F. Shkurti, "Taskography: Evaluating robot task planning over large 3D scene graphs," in *Conference on Robot Learning (CoRL)*. PMLR, Jan. 2022, pp. 46–58.
- [31] Y. Tian, K. Khosoussi, and J. P. How, "A resource-aware approach to collaborative loop-closure detection with provable performance guarantees," *Intl. J. of Robotics Research*, vol. 40, no. 10-11, pp. 1212–1233, Sep. 2021.
- [32] C. Denniston, Y. Chang, A. Reinke, K. Ebadi, G. Sukhatme, L. Carlone, B. Morrell, and A. Agha-mohammadi, "Loop closure prioritization for efficient and scalable multi-robot SLAM," *IEEE Robotics and Automation Letters (RA-L)*, 2022, (pdf).
- [33] D. T. Larsson, D. Maity, and P. Tsotras, "Q-Tree Search: An Information-Theoretic Approach Toward Hierarchical Abstractions for Agents With Computational Limitations," *IEEE Trans. Robotics*, vol. 36, no. 6, pp. 1669–1685, Dec. 2020.
- [34] —, "Information-theoretic abstractions for resource-constrained agents via mixed-integer linear programming," in *Proc. of the Workshop on Computation-Aware Algorithmic Design for Cyber-Physical Systems*, May 2021, pp. 1–6.
- [35] —, "Information-Theoretic Abstractions for Planning in Agents With Computational Constraints," *IEEE Robotics and Automation Letters*, vol. 6, no. 4, pp. 7651–7658, Oct. 2021.
- [36] —, "A Generalized Information-Theoretic Framework for the Emergence of Hierarchical Abstractions in Resource-Limited Systems," *Entropy*, vol. 24, no. 6, p. 809, Jun. 2022.
- [37] P. N. Klein, "A subset spanner for Planar graphs, with application to subset TSP," in *Proceedings of the Annual ACM Symposium on Theory of Computing*, ser. STOC '06, May 2006, pp. 749–756.
- [38] I. Althöfer, G. Das, D. Dobkin, D. Joseph, and J. Soares, "On sparse spanners of weighted graphs," *Discrete Comput Geom*, vol. 9, no. 1, pp. 81–100, Jan. 1993.
- [39] T. Kavitha, "New Pairwise Spanners," in *International Symposium on Theoretical Aspects of Computer Science (STACS 2015)*, vol. 30, 2015, pp. 513–526.
- [40] S. Baswana, T. Kavitha, K. Mehlhorn, and S. Pettie, "Additive spanners and (a,b)-spanners," *ACM Trans. Algorithms*, vol. 7, no. 1, pp. 5:1–5:26, Dec. 2010.
- [41] A. Abboud and G. Bodwin, "The 4/3 Additive Spanner Exponent Is Tight," *J. ACM*, vol. 64, no. 4, pp. 28:1–28:20, Sep. 2017.
- [42] M. Cygan, F. Grandoni, and T. Kavitha, "On Pairwise Spanners," in *International Symposium on Theoretical Aspects of Computer Science (STACS)*, vol. 20, Dagstuhl, Germany, 2013, pp. 209–220.
- [43] M. Elkin, Y. Gitlitz, and O. Neiman, "Almost Shortest Paths with Near-Additive Error in Weighted Graphs," in *Proc. of the Scandinavian Symposium and Workshops on Algorithm Theory (SWAT)*, vol. 227, 2022, pp. 23:1–23:22.
- [44] R. Ahmed, G. Bodwin, F. D. Sahneh, S. Kobourov, and R. Spence, "Weighted Additive Spanners," in *Graph-Theoretic Concepts in Computer Science*, ser. Lecture Notes in Computer Science, 2020, pp. 401–413.
- [45] R. Ahmed, G. Bodwin, F. D. Sahneh, K. Hamm, S. Kobourov, and R. Spence, "Multi-Level Weighted Additive Spanners," in *Proc. of the International Symposium on Experimental Algorithms (SEA)*, vol. 190, 2021, pp. 16:1–16:23.
- [46] K. Censor-Hillel, T. Kavitha, A. Paz, and A. Yehudayoff, "Distributed construction of purely additive spanners," *Distrib. Comput.*, vol. 31, no. 3, pp. 223–240, Jun. 2018.
- [47] S. Baswana and S. Sarkar, "Fully dynamic algorithm for graph spanners with poly-logarithmic update time," in *Proc. of the Annual ACM-SIAM Symp. on Discrete Algorithms (SODA)*, Jan. 2008, pp. 1125–1134.
- [48] S. Arya, G. Dast, D. M. Mount, J. S. Salowe, and M. Smid, "Euclidean spanners: Short, thin, and lanky," in *Proc. of the Acm Symposium on Theory of Computing*, 1995, pp. 489–498.
- [49] A. Abboud and G. Bodwin, "Reachability Preservers: New Extremal Bounds and Approximation Algorithms," in *Proc. of the Annual ACM-SIAM Symp. on Discrete Algorithms (SODA)*, Jan. 2018, pp. 1865–1883.
- [50] N. Tishby, F. Pereira, and W. Bialek, "The information bottleneck method," *Proc. of the Allerton Conference on Communication, Control and Computation*, vol. 49, 07 2001.
- [51] A. Rosinol, A. Violette, M. Abate, N. Hughes, Y. Chang, J. Shi, A. Gupta, and L. Carlone, "Kimeria: from SLAM to spatial perception with 3D dynamic scene graphs," *Intl. J. of Robotics Research*, vol. 40, no. 12–14, pp. 1510–1546, 2021, arXiv preprint arXiv: 2101.06894, (pdf).

APPENDIX A
EXACT BUDGET-CONSTRAINED SPANNER

Problem (1) can be solved exactly by the following ILP (adapted from the exact spanner formulation in [45, Section 4]),

$$\min_{\substack{\beta \\ x_i \forall i \in \mathcal{V}_G \\ x_{i,j}^{st} \forall (i,j) \in \mathcal{E}_G, \forall (s,t) \in \mathcal{P}}} \beta \quad (5a)$$

$$\text{s.t.} \quad \sum_{(i,j) \in \bar{\mathcal{E}}_G} x_{(i,j)}^{uv} W^G(i,j) \leq d_G(s,t) + \beta W_{\max}^G(s,t) \quad \forall (s,t) \in \mathcal{P}, \forall (i,j) \in \mathcal{E}_G, \quad (5b)$$

$$\sum_{(i,j) \in \text{Out}(i)} x_{(i,j)}^{st} - \sum_{(j,i) \in \text{In}(i)} x_{(j,i)}^{st} = \begin{cases} 1 & i = s \\ -1 & i = t \\ 0 & \text{else} \end{cases} \quad \forall (s,t) \in \mathcal{P}, \forall i \in \mathcal{V}_G, \quad (5c)$$

$$\sum_{(i,j) \in \text{Out}(i)} x_{(i,j)}^{st} \leq 1 \quad \forall (s,t) \in \mathcal{P}, \forall i \in \mathcal{V}_G, \quad (5d)$$

$$x_i \geq x_{(i,j)}^{st} + x_{(j,i)}^{st} \quad \forall (s,t) \in \mathcal{P}, \forall i \in \mathcal{V}_G, \forall (i,j) \in \mathcal{E}_G, \quad (5e)$$

$$\sum_{i \in \mathcal{V}_G} x_i \leq B, \quad (5f)$$

$$x_i, x_{(i,j)}^{st} \in \{0, 1\} \quad \forall (s,t) \in \mathcal{P}, \forall i \in \mathcal{V}_G, \forall (i,j) \in \mathcal{E}_G, \quad (5g)$$

where x_i is associated with each node $i \in \mathcal{V}_G$ and is 1 if it is included in the spanner, $x_{(i,j)}^{st}$ is an edge variable equal to 1 if and only if edge (i,j) is taken as part of the path between s and t , $\bar{\mathcal{E}}_G$ is the augmented set of bidirected edges, obtained by adding edge (j,i) for each edge $(i,j) \in \mathcal{E}_G$, (5b) forces maximum distortion for all paths between terminal nodes, (5c)–(5d) ensure that the chosen edges form a path for each pair of terminals (s,t) , (5e) ensures that a node i is taken if any edges incident to it are taken, and (5f) encodes the limited budget on the number of selected nodes.

APPENDIX B
CALCULATION OF EDGE WEIGHTS

The edge weights associated with the intra-layer edges of the 3D Scene Graph \mathcal{G} are simply the Euclidean distance between the two nodes the edge connects. For example, for the layer consisting of places, the weight associated to an edge would be the Euclidean distance between the two connected places; for the layer consisting of rooms, the edge weight would be the Euclidean distance between the centroid of two rooms. The calculation of inter-layer edge weights is more nuanced: they cannot be simply Euclidean distances, since that would fail to capture the actual effort to traverse, for example, from a room centroid to a place in the room without precise knowledge of free-space locations in the place layer. Intuitively, the lack of such precise spatial information requires the robot to parse the room by locally exploring it, until the target location (place) is reached. In general, if the robot is aware only of an abstract, spatially coarse representation of granular geometric information about free-space locations (such as a room or building node that represents a set of places nodes), time-consuming exploration is needed to supply the missing spatial information. This fact well summarizes the trade-off that a robot faces when compressing its local map: high compression rate enables quicker transmission, but inevitably causes the robot that receives the compressed map to perform suboptimal navigation.

Hence, for inter-layer edges, we devise a method to associate to each edge a weight that is at least as large as the shortest path of traversal. In particular, for each inter-layer edge, we have a node in the higher layer, denoted by \mathbf{x} , and a node in the lower layer, denoted by \mathbf{y} . To find the weight of the inter-layer edge $e_{\mathbf{x},\mathbf{y}}$ connecting \mathbf{x} and \mathbf{y} , we first find a node \mathbf{y}_0 in the lower layer that has the smallest Euclidean norm to the centroid of the set of all the nodes that are children of \mathbf{x} : then, the weight of $e_{\mathbf{x},\mathbf{y}}$ is computed as

$$W^G(\mathbf{x}, \mathbf{y}) \doteq \|\mathbf{x} - \mathbf{y}_0\| + d_G(\mathbf{y}_0, \mathbf{y}), \quad (6)$$

where $\|\cdot\|$ denotes the Euclidean norm. Observe that the weight is greater than or equal to the path length of the shortest path between \mathbf{y}_0 and \mathbf{y} . Intuitively, the weight of a room-to-place inter-layer edge is the distance between the room centroid and the closest place, plus the path length from the closest place to the target place.

Importantly, the above heuristic is consistent with navigation performance: the cost (*i.e.*, estimated navigation time) of traversing the inter-layer edge between two nodes (*e.g.*, to navigate from a place node to the room centroid) is higher than following the shortest path on the place layer that connects the two corresponding place nodes (*e.g.*, the source place node and the closest place node to the room centroid). This feature is crucial in order for the proposed compression algorithms to work

properly, because they will first favor intra-layer edges (which retain navigation performance) and use inter-layer edges only when necessary (causing an increase in navigation time).

However, we also note that calculating the actual impact of local navigation is difficult having only the final DSG, so that the actual navigation time may differ from the estimated one. Nonetheless, we argue that such inter-layer edge weights could be reliably estimated by a robot navigating the environment. Indeed, rather than calculating the weights *a posteriori* based on the final DSG, the robot can compute them *online* (while building the DSG) based on its own exploration time: this directly relates inter-layer edges between places, rooms, and buildings nodes with the expected navigation effort.

APPENDIX C EXTRA NUMERICAL TESTS AND SIMULATIONS RESULTS

In this Appendix, we visually illustrate how the proposed algorithms perform on two tested simulated environments: an apartment scene and the office scene already used in Section V.

A. Apartment Scene

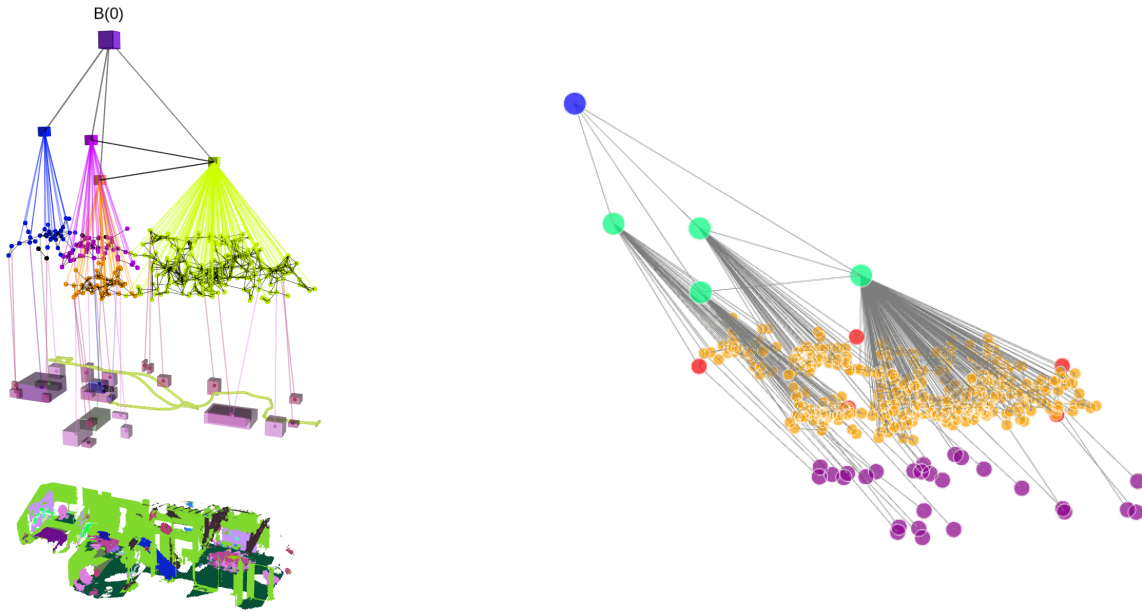


Figure 6: Original 3D Scene Graph of the Apartment scene. Left: full DSG with semantic map and meshgrid. Right: schematic version with objects (purple), places (yellow), rooms (green), and building (blue) nodes. Terminal places nodes are marked with red color. Full size: 453 nodes.

Figure 6 shows the original DSG of the Apartment, which is composed of 453 nodes connected by 1403 edges.

Figure 7 shows the compressed graphs obtained by running BUD-Lite with different budget values. Recall that BUD-Lite compressed the DSG by exploiting the hierarchy bottom-up, parsing shortest paths one after the other and abstracting away places nodes to their corresponding room nodes. In this case, we consider four terminals nodes scattered across three rooms. Note that, as the available budget decreases (*i.e.*, the communication constraint get tighter), portions of shortest paths along places nodes are pruned away and abstracted into their respective room nodes. In particular, BUD-Lite uses a single room node when the budget is 30 (Fig. 7a) or larger (Fig. 7b), sacrificing navigation performance for the two terminals nodes belonging to that room and retaining fine-scale spatial information in proximity of the two terminals nodes belonging to other two rooms. Conversely, all rooms are used when the budget gets too small (Fig. 7c), and the compression procedure is forced to remove all free-space locations in the place layer. Importantly, the output of BUD-Lite also depends on the order in which terminals pairs (and hence shortest paths) are parsed, which may cause larger or smaller amounts of nodes to be deleted before others: improving this feature of the algorithm is an important aspect that will be considered in follow-up work.

Conversely, TOD-Lite results are shown in Fig. 8. Recall that this algorithm leverages the DSG hierarchy via top-down expansion of nodes, which is clearly visible from Fig. 8 as opposed to shortest path-wise compression on BUD-Lite. In particular, it can be seen from Figs. 8a and 8b that expanding one room node is not possible without exceeding the allowed budget: hence, TOD-Lite expands the other two rooms nodes in both cases, resulting in preserved places nodes close to the two terminals

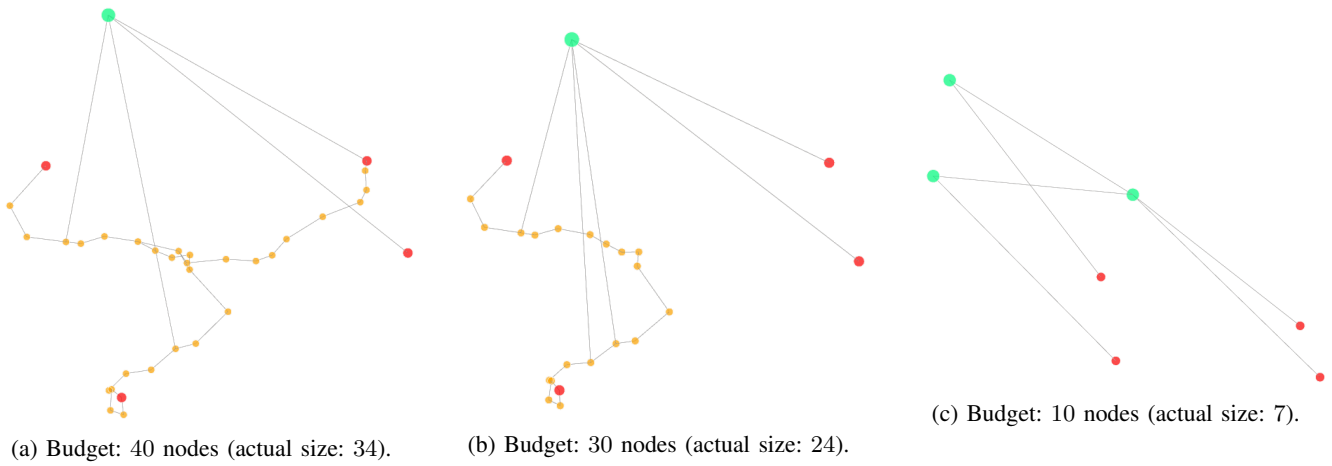


Figure 7: Compressed 3D Scene Graph of the Apartment output by BUD-Lite.

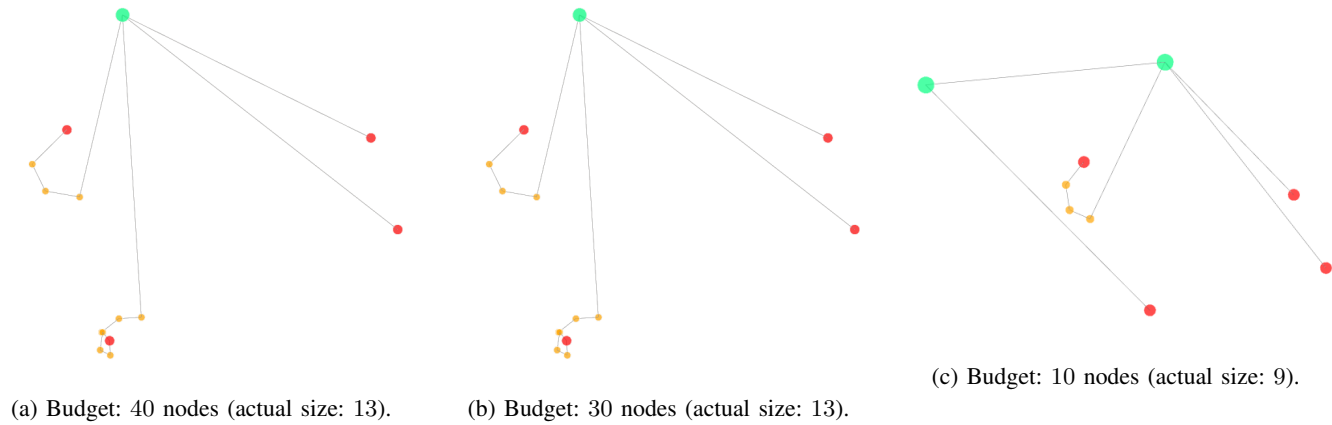


Figure 8: Compressed 3D Scene Graph of the Apartment output by TOD-Lite.

nodes on the left. When budget is further reduced (Fig. 8c), two rooms are not expanded and fine-scale geometric information in the place layer is retained only for the room corresponding to the terminal node on the top left.

Comparing the compression results of BUD-Lite in Fig. 7 and of TOD-Lite in Fig. 8 shows both their different mechanisms and advantages: in this case, large budgets favor the BUD-Lite bottom-up compression, which is able to retain more places nodes; instead, small budget favors the TOD-Lite top-down expansion, which eventually retains places nodes associated with one room, whereas the order chosen to parse shortest paths in the BUD-Lite forces to abstract away all nodes in the place layer.

B. Office Scene

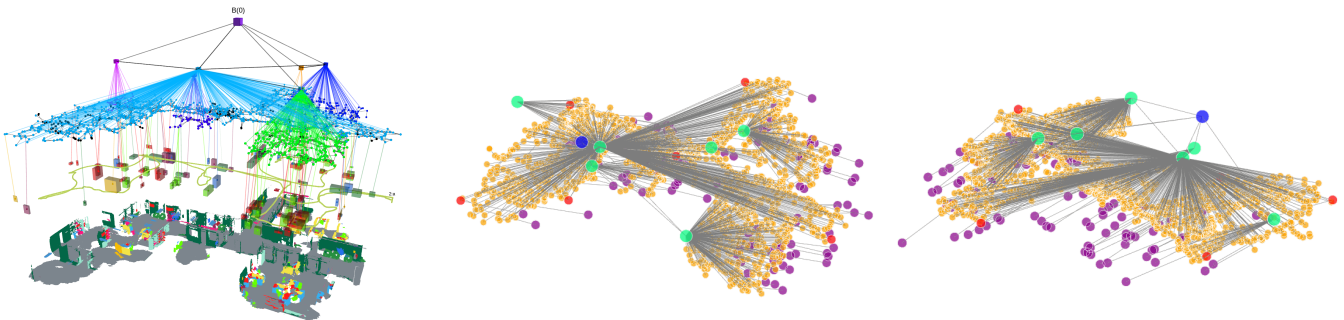


Figure 9: Original 3D Scene Graph of the Office scene. Left: full DSG with semantic map and meshgrid. Right: schematic version. Full size: 1675 nodes.

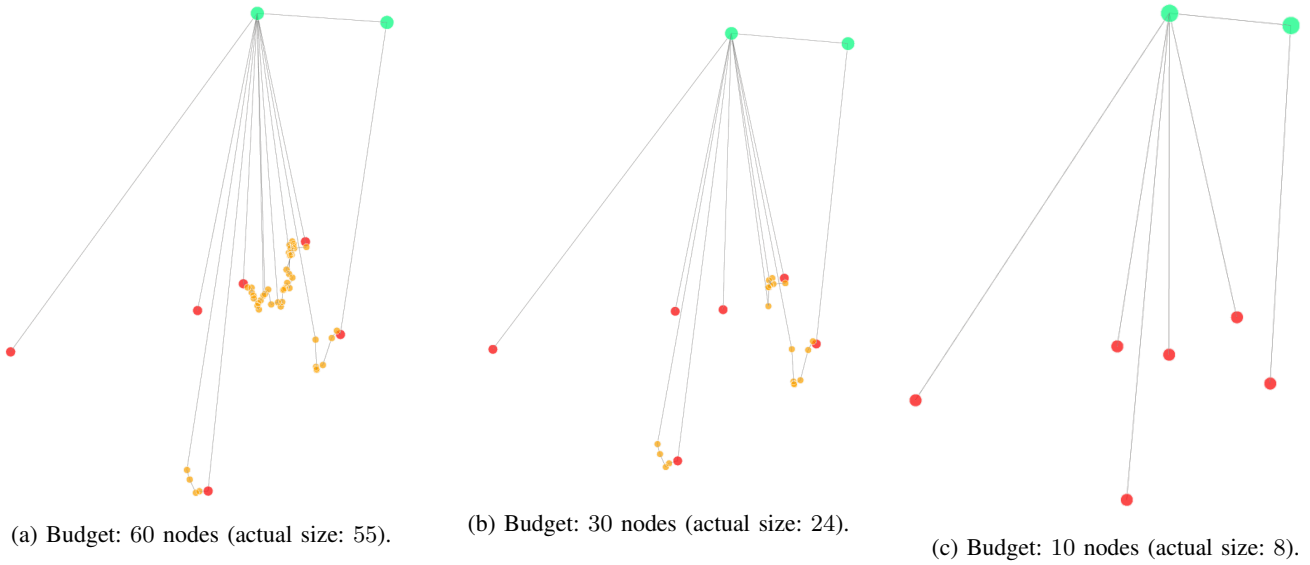


Figure 10: Compressed 3D Scene Graph of the Office output by BUD-Lite.

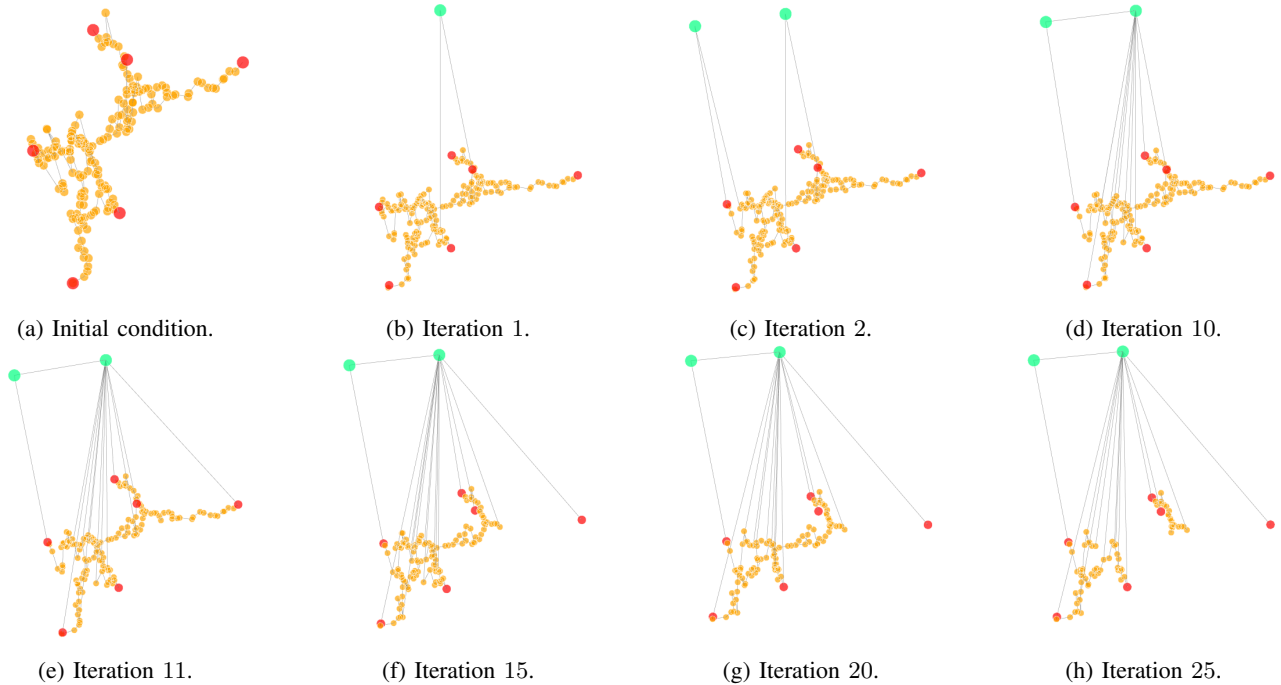
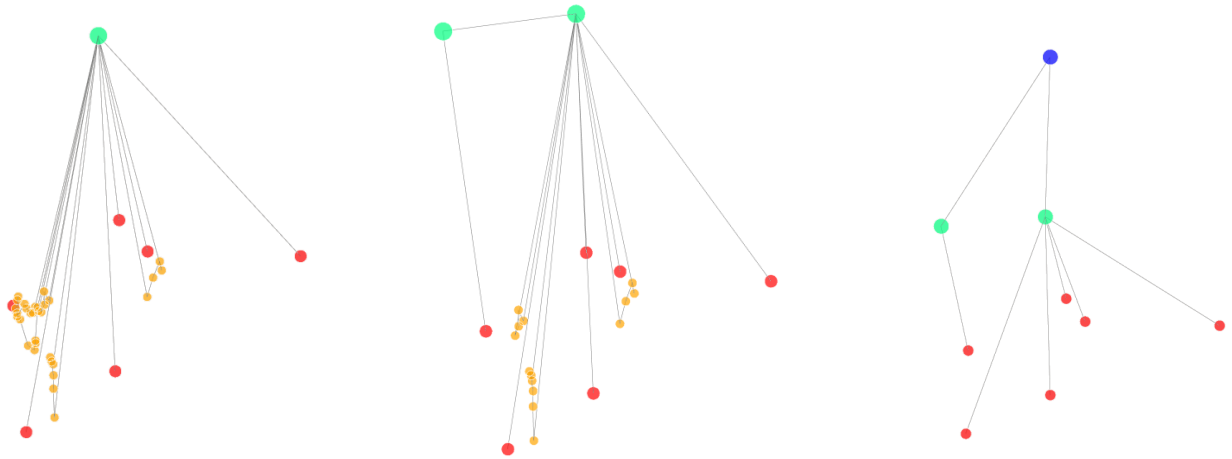


Figure 11: Iterations of the bottom-up compression phase of BUD-Lite (budget: 60 nodes).

Figure 9 shows the original DSG of the Office, which is composed of 1675 nodes connected by 5396 edges. For this test, we consider six terminal nodes scattered across two rooms.

Figure 10 shows the compressed graphs output by BUD-Lite. The same general remarks carried out before also apply here. Notably, one of the interested rooms (gathering five out of the six terminals nodes) is very large (it is in fact a corridor, see Fig. 9), which may cause the compression procedure of BUD-Lite to act in too unbalanced fashion if the portions of shortest paths passing through that room are abstracted away at once. To improve granularity of compression in this case, we forced a maximum number of places nodes that can be compressed within a single iteration (corresponding to a slight modification to the condition of Line 8 of Algorithm 2): in particular, we set 20 places nodes as maximum threshold, so that long stretches of places nodes are compressed at a pace of 20 (or fewer) at each iteration.

Figure 11 shows the breakdown of some iterations of the compression procedure carried out within the BUD-Lite algorithm, corresponding to the loop at Line 7 of Algorithm 2. The initial condition shown in Fig. 11a corresponds to the spanner output



(a) Budget: 60 nodes (actual size: 38).

(b) Budget: 30 nodes (actual size: 22).

(c) Budget: 10 nodes (actual size: 9).

Figure 12: Compressed 3D Scene Graph of the Office output by TOD-Lite.

by `build_spanner` in Line 1. Note that the latter is composed of only places nodes, and rooms nodes abstractions are introduced by subsequent compression iterations. Specifically, one room is added at the first iteration (Fig. 11b) and the other, which is connected to the first room, at the second iteration (Fig. 11c). Shortest paths are parsed one after the other, which causes places nodes to be retained until there is no path using them: for example, the inter-layer edge between the rightmost terminal node and its associated room node is added at iteration 11 (Fig. 11e), but the corresponding stretch of places nodes is removed only at iteration 15 (Fig. 11f), when all shortest paths with source the rightmost terminal node have been parsed and shortcut through the room. The output compressed DSG in Fig. 10a is obtained after 28 iterations.

Figure 12 shows the compressed graphs output by TOD-Lite. The same general remarks carried out for the Apartment also apply here. In particular, note that the small budget of 10 nodes in this case prevents TOD-Lite to perform any expansion, see Fig. 12c.